ELSEVIER Solar Energy Materials and Solar Cells 52 (1998) 399–411

Solar Energy Materials & Solar Cells

Photoelectrochemical behavior of chemically deposited CdSe and coupled CdS/CdSe semiconductor films

M.E. Rincón*, M. Sánchez, A. Olea, I. Ayala, P.K. Nair

Photovoltaic Systems Group, Laboratorio de Energía Solar-IIM, Universidad Nacional Autónoma de México, Temixco 62580, Morelos, Mexico

Abstract

Photoelectrochemical effects at chemically deposited CdSe thin films (2000 Å) coupled with as-prepared and air annealed (250°C) CdS films have been investigated by monitoring open-circuit voltage (V_{oc}) and short-circuit current density (I_{sc}) at varying incident light intensities and for different heat-treatments temperatures. Two consecutive chemical baths were used in the coupled system. Each bath has been optimized in earlier studies for the deposition of highly photosensitive CdS and CdSe thin films. The photoelectrochemical behavior of single and coupled films was investigated in ferricyanide redox couples. The enhanced short-circuit photocurrent of the as-deposited CdS/CdSe system, despite their lower photosensitivity, indicated that charge separation improved in the coupled system. The role of post-deposition thermal treatments in improving the photoelectrochemical cell characteristics and stability of coupled semiconductors was investigated. Excellent I–V properties were obtained for CdSe and CdS_{250}/CdSe photoelectrodes annealed at 280°C. For the coupled system: $V_{oc} = 960$ mV; $I_{sc} = 8.6$ mA/cm^2; fill factor (ff) = 0.53 and cell efficiency (η) = 4.2%. The linearity of $V_{oc}/\ln(I_L)$ and I_{sc}/I_L plots supports the Schottky–Mott model for these interfaces. The stability of the coupled photoanode is superior to that of the CdSe only-film for the initial 3 h.

Keywords: Thin films; Phtoelectrochemical effects; Open-circuit voltage; Short-circuit current density

* Corresponding author.

PII S0927-0248(97)00238-9

1. Introduction

The essential features of an ideal semiconductor material for regenerative PECs have been summarized elsewhere [1]: stable against photocorrosion, sensitive in the visible spectrum, valence band (photoanodes) or conduction band (photocathodes) close to the equilibrium potential of the required electrolytic reactions, and electrocatalytic surface to ensure fast charge transfer. Due to the incompatibility of some of these features (wide band-gap semiconductors have remarkable stability against photocorrosion but they are only ultraviolet-sensitive and therefore inefficient in its response to the solar spectrum) research efforts have switched from the search for this ideal material to the development of structures of compatible materials, each optimized for a particular function. This new approach has to consider the fact that the charge separation mechanism might be controlled by factors other than the space charge layer at the semiconductor-electrolyte interface [2]. In addition to this, the polycrystalline nature of many semiconductor films causes a high density of surface states which make the shifts in flat band potentials caused by redox species difficult to predict and hence not included in the models based on depletion layer theory [3,4]. Consequently, we rely heavily on experimental techniques to characterize and validate the use of these structures on PEC systems.

In the above framework of research efforts, photoanodes of CdS/CdSe have been developed in our laboratory using chemical deposition technique. This method is very attractive for producing large area electrodes and has gained renewed interest due to the good quality of the deposited films and the possibility of enhancing photosensitivity and inducing n- or p-type character in many metal chalcogenides through thermal treatments at relatively low temperatures, 200°–400°C [5–7]. The applicability in PEC systems of chemically deposited CdS and CdSe have been explored by several research groups. PEC systems using chemically deposited CdSe films with excellent prospects were reported by the group of Rauh [8,9] and Savadogo and Mandal [10,11]. Efficiencies as high as 6.8% [8,9] and 11.7% [10,11] have been reported for these systems, achieved through in situ surface modification and the use of counter electrodes based on p-type materials (CoS and CuS). PEC systems utilizing chemically deposited CdS films were reported by Chandra et al. [12], Lokhande and Pawar [13,14], and Gotovac and his coworkers [4,15,16]. The highest efficiency for these systems was 1.53% [4]. The PEC behavior of coupled systems of CdS/CdSe have been reported by Mahapatra and Dubey [17]. In this system, however, the CdS substrate was a pressure-sintered or electrodeposited film and the CdSe film was produced by anion exchange ($S^{2-} + Se \rightarrow Se^{2-} + S$) in a chemical bath containing only the selenizing source. The efficiency reported for this particular system was in the range of 2.7–4.5%.

In the present work we report the PEC behavior of thin CdSe and coupled CdS/CdSe semiconductor films obtained by chemical deposition. The coupled film was obtained from two consecutive baths. Each bath has been optimized in earlier studies [5–7] for the deposition of highly photosensitive CdS and CdSe films. Due to the thin film nature and polycrystallinity of the CdSe films, the possibility of a charge separation mechanism controlled by the rectifying junction of CdS/CdSe films instead

of the space charge layer at the CdSe/electrolyte interface was examined. The role of post-deposition thermal treatment in improving the photocurrent stability and cell efficiency was also studied.

2. Experimental

2.1. Chemical deposition

The chemical deposition technique for CdS thin films has been reported before [7]. A 100 ml volume of the deposition mixture was prepared by the sequential addition of the following: 3 ml of 1 M cadmium nitrate, 12 ml of 1 M sodium citrate, 10 ml of 4 M NH_3 (aq), 5 ml of 1 M thiourea and 70 ml of deionized water.

Microscope glass slides (75 mm × 25 mm × 1 mm) and stainless steel slides of the same dimensions were used as substrates. The glass slides were washed with detergent solution and rinsed with de-ionized water prior to the deposition of the films. The stainless steel slides were degreased with acetone and washed with detergent solution. The clean slides were placed vertically on the walls of the 100 ml beaker containing the deposition mixture. The CdS films were deposited at 50°C for 24 h. The films were uniform and showed the familiar complex morphology characteristic of long duration of deposition: compact inner layer and porous outer layer [18,19].

For the deposition of CdSe thin films, the source of selenide ions was a freshly prepared solution of sodium selenosulfate. The stock solution of this reactive was prepared as follows: 12.5 g of sodium sulfite and 4 g of selenium powder were introduced into a 250 ml conical flask containing 100 ml of de-ionized water. The mixture was stirred and refluxed at 90°C for 5–6 h after which it was filtered resulting in a clear solution of sodium selenosulfate of approximately 0.45 M concentration. A 100 ml chemical bath for the deposition of CdSe films was prepared by the addition of the following: 3 ml of 1 M cadmium nitrate, 4 ml of 1 M TEA, 2.5 ml of 15.2 M NH_3 (aq), 3 g of sodium sulfite, 7 ml of 0.45 M selenosulfate and deionized water. The CdSe films were deposited on glass and stainless steel substrates with and without chemically deposited CdS. To investigate the influence of the CdS substrate, two series of coupled films were developed: (i) CdSe films deposited on CdS without thermal treatment (CdS/CdSe series), (ii) CdSe films deposited on CdS annealed in air at 250°C for 1 h (CdS_{250}/CdSe series). The deposition of CdSe films was done at 80°C during 3 h and in three consecutive baths. Each bath adds a compact CdSe film of about 0.1 μm thickness.

Air annealing of the films was done at atmospheric pressure for 1 h each at the chosen temperatures (200–420°C) in a Thermolyne 1500 furnace.

2.2. Optical and electrical characterization

The optical and electrical characterization was done on films deposited on glass substrates. The thicknesses of the as-deposited and air annealed films were determined

using an Alpha Step 100 unit. Thickness measurements could not be made satisfactorily on films deposited on stainless steel due to its roughness. The optical transmittance and reflectance spectra of the films were recorded using a Shimadzu UV-3101PC spectrophotometer for film side incidence and with air as reference. To study the photosensitivity of the films, a Keithley 619 Electrometer and Keithley-Voltage Source was interfaced to a PC-XT. Pairs of silver-paint electrodes of 5 mm length at 5 mm separation were printed on the surface of the film and a bias of 10 V applied across them. The measurement of photocurrent was done under 600 W/m^2 tungsten halogen illumination during 20 s in the dark, 20 s under illumination and 20 s in the dark decay mode. The recording started after samples reached steady-state current conditions in the dark.

2.3. PEC characterization

The PEC cell had a single compartment consisting of the semiconductor photoelectrode (films deposited on the stainless steel substrate) and a large graphite counter electrode. Freshly prepared ferro/ferricyanide and polysulfide systems were used as the working redox electrolytes. A copper lead was attached to the stainless steel by means of Sn soldering and silicone glue and then enclosed in a glass tube. Silicone was also used to seal the edges of the glass tube and to insulate the back contact and the stainless steel from the electrolyte leaving only 1 cm^2 of the semiconductor film in contact with the electrolytic solution. The I–V curve of stainless steel–copper/tin junction indicated ohmic nature. The PEC cell was illuminated with a 100 W tungsten-halogen lamp. The illumination intensity was measured using a calibrated Si photodiode. The intensity of illumination was varied (40–100 mW/cm^2) by varying the distance between the lamp and the PEC cell. All experiments were performed at room temperature and under nitrogen bubbling, which also provided adequate stirring of the electrolyte. Current–Voltage (I–V) curves were obtained using a computerized system consisting of : Keithley 230 Programmable Voltage Source, Keithley 619 Electrometer/Multimeter and a PC-XT.

3. Results and discussion

The effect of annealing temperature on film thickness is shown in Fig. 1. The thickness of the as-prepared CdSe film was ~ 0.25 μm and does not vary significantly with air annealing in the temperature range of 25–380°C. In contrast, the thickness of the as-deposited CdS film was 1.7 μm and decreases with increasing annealing temperature. The thickness of the as-prepared coupled film was higher in the film deposited on CdS without thermal treatment. The difference amounts to a thickness reduction by 0.2 μm of the as-prepared CdS film when heated at 250°C. The thickness of the coupled films (0.95–1.15 μm) does not correspond to the sum of the thicknesses of the individual films obtainable from the independent baths ($t_{CdS} + t_{CdSe}$). A CdS layer of at least 0.55 μm thickness is dissolved prior to the deposition of the CdSe film. This dissolution occurs probably in the porous top layer of the CdS film at the higher

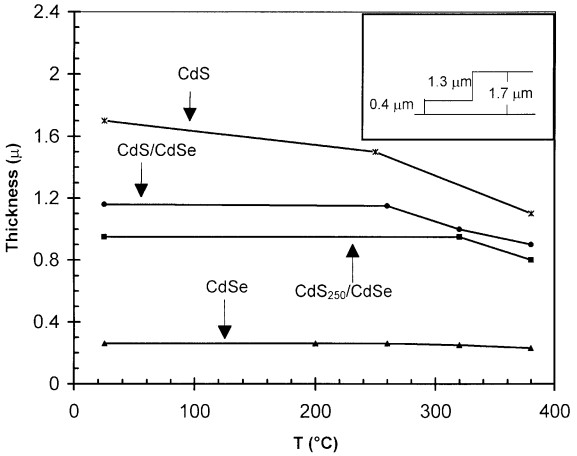

Fig. 1. Effect of annealing temperature on film thickness for chemically deposited CdS, CdSe and coupled films: CdS/CdSe and CdS_{250}/CdSe. The insert shows the complex morphology of the as-prepared CdS. The chemically deposited films were air annealed for 1 h at the specified temperature.

deposition temperature ($T_{dep} = 80°C$) of the CdSe bath. This dissolution takes place to the same extent in as-prepared and annealed CdS films. The inset in Fig. 1 shows the typical composition of a typical CdS thin film arrived at from thickness determination: 0.4 μm of compact layer and 1.3 μm of porous layer. It is apparent in Fig. 1 that most of the porous layer is probably removed by thermal treatments and dissolution prior to the deposition of the CdSe film. Coupled films obtained by depositing CdSe films on annealed CdS films show smaller variation in thickness with further annealing.

The dark current (I_{dark}) and photosensitivity (S) of the films as a function of annealing temperature are given in Fig. 2a and Fig. 2b. The photosensitivity is defined as $S = (I_{photo} - I_{dark})/I_{dark}$, where I_{photo} is the electrical current under illumination. In previous work [6,7] air annealing of the chemically deposited CdS and CdSe films has been shown to improve dramatically the photosensitivity of the films. The presence of adsorbed/chemisorbed oxygen in the annealed films (no oxides were identified by XRD but an appreciable amount of O was determined by XPS) was thought to be responsible for the improvement in photosensitivity which is in agreement with the well established theory of photoconductivity of polycrystalline thin films [20,21]. That is, a negatively charged intergrain region containing the chemisorbed oxygen gives rise to an intergrain barrier that causes an exponential decrease in the electrons drift mobility (low conductivity in the dark). Under illumination, the negatively charged region gets neutralized by the photogenerated holes leading to a reduction in the intergrain potential barrier and hence to an enhancement of the electron drift mobility (high conductivity under illumination). A maximum in photosensitivity is expected at annealing temperatures in which the growth of the

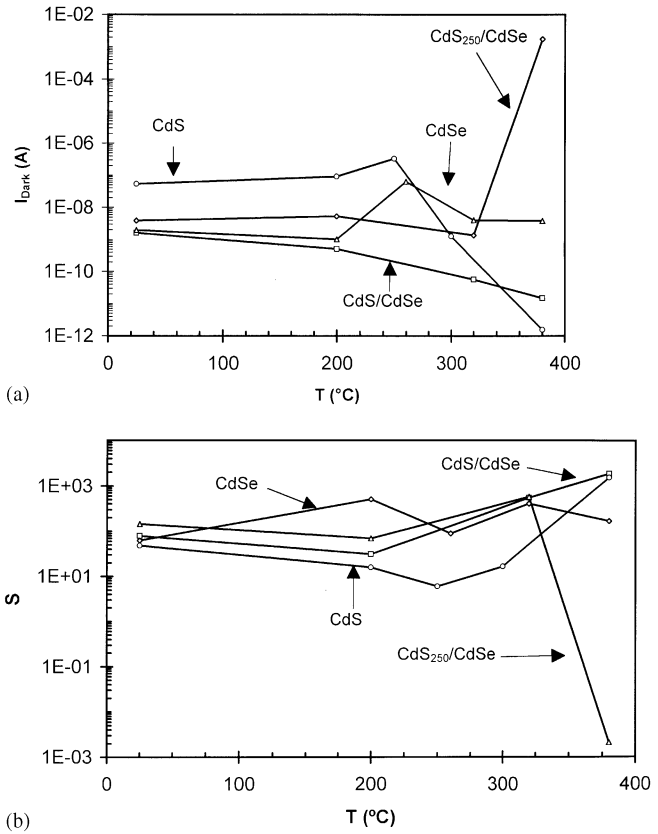

Fig. 2. Electrical characterization of chemically deposited CdS, CdSe and coupled films as a function of annealing temperature. (a) Dark current (I_{dark}), (b) Photosensitivity (S) = $(I_{photo} - I_{dark})/I_{dark}$. Annealing in air for 1 h.

grain itself causes an increase in the dark conductivity due to the reduction in the number of intergrain barriers. In both, CdSe and CdS films, S drops substantially at temperatures in which conversion to oxides species is expected to be promoted. Fig. 2a shows the high resistivity of the as-prepared CdSe film (I_{dark} two orders of magnitude lower than the CdS film) which cannot be accounted for the difference in their thickness (a factor of 6). Furthermore, the resistivity of the as-prepared coupled films is determined by the CdSe component and is slightly sensitive to the thermal treatment of the CdS substrate. As expected, air annealing decreases the dark conductivity in CdS films due to oxygen chemisorption. In these films, I_{dark} decreases in the temperature range of 250–380°C and at 420°C (not shown) abruptly increases (conversion to oxides). In the case of CdSe, the pattern shows an overall increase in I_{dark} with annealing temperature and a maximum at 260°C. The resistivity of the coupled films is lower for the CdS_{250}/CdSe series which stays relatively constant for

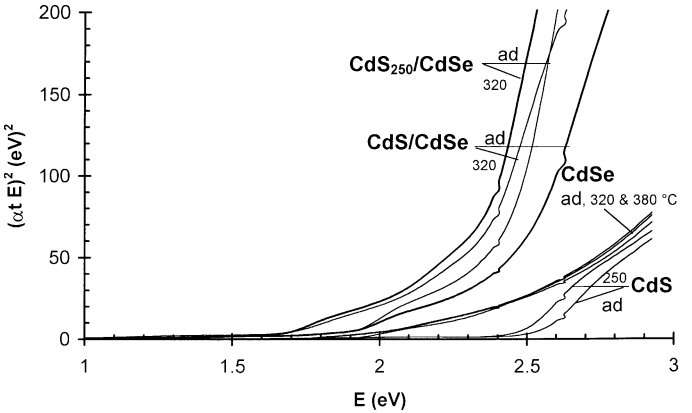

Fig. 3. Plots of $(\alpha thv)^2$ vs. hv of the as-prepared and thermally treated CdS, CdSe and coupled films.

thermal treatments up to 320°C. Annealing at 380°C increases the conductivity by almost 6 orders of magnitude. This high value is likely to be due to oxidation of the inner CdS layer. On the contrary, annealing of the CdS/CdSe series shows a continuous decrease in dark current, partly due to thickness reduction, which indicates that the CdSe layer acts as a protecting layer and it is the chemisorbed oxygen already present in the annealed CdS substrate which causes oxidation. It is interesting to note that there is a shift in oxidation temperatures of CdS films ($T_{ox} = 420$°C) and CdS_{250}/CdSe films ($T_{ox} = 380$°C). A shift to higher temperatures is expected in the oxidation of thicker films due to oxygen diffusion mechanisms [22]. Therefore, the higher oxidation temperature of CdS is consistent with its higher thickness. The strong dissolution of the CdS film prior to the deposition of CdSe suggests the possibility of formation of a truly ternary compound CdS_ySe_{1-y} in the outer layer, in which case the photosensitivity results will be determined by the stoichiometry and chemical stability of this film. Fig. 2b shows the expected increase in photosensitivity with annealing temperature for CdS. The coupled CdS_{250}/CdSe series has its maximum value of photosensitivity at annealing temperature of 320°C, above which S drops substantially due to oxidation. The coupled CdS/CdSe series show a substantial increase in photosensitivity in the temperature range tested, while the photosensitivity of CdSe films stays relatively constant.

The band gap (E_g) of the films was determined from the equation describing optical absorption of direct transitions in crystalline materials. Fig. 3 shows plots of $(\alpha t\ hv)^2$ vs. (hv) for the coupled films and for the individual binary components. Here "α" is the absorption coefficient, "t", the thickness of the absorbing layer and "hv", the photon energy. The product αt was obtained from transmittance spectra after correcting for front surface reflection [23]. In this figure the contribution of the CdS and CdSe components in the optical absorption of the coupled film is evident: two linear regions and two crossings of the energy axis are indicative of a solid mixture [23]. It is also seen that E_g shifts to lower energies when the coupled films are annealed and that the

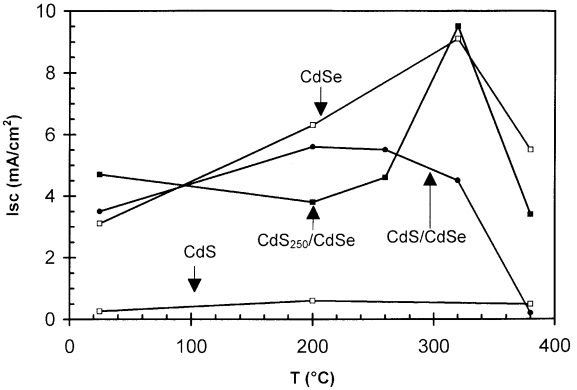

Fig. 4. I_{sc} (short circuit current density) as a function of annealing temperature for CdS, CdSe and coupled photoanodes. PEC cell formed by: semiconductor | 0.5 M KOH/0.25 M $K_4Fe(CN)_6$/0.0125 M $K_3Fe(CN)_6$ |C. 100 W tungsten-halogen lamp at an intensity of 80 mW/cm^2.

absorption coefficient is larger for annealed coupled films, specially for films of the series CdS_{250}/CdSe. The lowest E_g for the CdS component was 2.3 eV and was obtained in samples of the CdS_{250}/CdSe series annealed at 320–380°C. The low response of CdS films at energies below 2.3 eV and the relatively high E_g ($\sim$ 1.9 eV compared with 1.75 eV for bulk material) of CdSe films even with thermal treatments of 380°C are characteristics features of the binary films. On the other hand, the contribution of the CdSe component in the coupled films suggests E_g in the range of 1.65–1.85 eV. The lowest value of E_g was obtained with samples of the series CdS_{250}/CdSe annealed at 320–380°C.

Fig. 4 shows the short circuit current densities (I_{sc}) of the PEC cells formed by the binary and coupled films and the ferro/ferricyanide system under 80 mW/cm^2 illumination, given as a function of annealing temperature. Preliminary testing with polysulfides and ferro/ferricyanides redox systems indicated the superior response of the latter redox couple when the CdSe film was in contact with the electrolyte. In Fig. 4 we can see that among the as-prepared films, the coupled systems give higher I_{sc} values, closely followed by CdSe. This behavior correlates well with the absorption edge of the films given in Fig. 3: lower the E_g, higher is the I_{sc}. The fact that the as-deposited coupled films and the CdSe films are highly resistive and with low photosensitivity when compared to the as-deposited CdS film does not seem to be important in determining I_{sc} (I_{sc} for CdS photoanodes was less than 1 mA/cm^2). It is well known that under the space charge layer model I_{sc} is determined by the generation and separation of the photogenerated carriers in the depletion zone (where the electric field exist). For this, the space charge layer thickness should be equal to or larger than the light absorption depth to assure rapid carrier separation. This thickness is inversely proportional to the square root of the donor density. Therefore, the combination of an n-type semiconductor with good electron mobility (CdS) and the almost intrinsic absorbing layer of CdSe, warrants strong carrier production with

few losses due to recombination. The effect of heat-treatment temperature on I_{sc} is difficult to predict, specially on coupled films, since several important parameters are subject to changes. It is interesting, however, to notice that most of the properties presented in Figs. 1–3 involved the bulk of the film, while I_{sc} and V_{oc} (open circuit voltage) are mainly determined by surface phenomena. For air annealed CdS films I_{sc} is almost constant with respect to annealing temperature regardless of the fact that the thickness, dark conductivity and photosensitivity of the films undergo important changes (Figs. 1–3). On the other hand, CdSe films annealed up to 320°C, show a trend towards increasing I_{sc} even though most of its properties (including αt and E_g) are almost constant. The coupled films show an interesting trend with respect to annealing temperature: their I_{sc} values are similar and relatively constant up to 260°C but at 320°C I_{sc} substantially grows for the annealed CdS_{250}/CdS film while slightly decreases for the annealed CdS/CdSe film. At this temperature the thickness and photosensitivity of the two series are similar and differences exist in dark conductivity and absorption coefficients at energies above 2 eV leading to films with higher I_{sc}. Surface defects at these temperatures could cause recombination problems in the thin CdSe layer and might explained the difference in I_{sc} of the coupled films and the subsequent drop of I_{sc} at 380°C. The oxidation of the CdS_{250}/CdSe film annealed at 380°C does not seem to be relevant in determining I_{sc}, because it affects only the inner layer making it more n-type. Oxygen chemisorption on the outer CdSe layer is probably more important at these temperatures. Thickness is another variable which strongly diminishes at 380°C and must be correlated to the decreased in I_{sc}. Further, loss of chalcogenides (S and Se), probable at high annealing temperature (380°C), will increase the n-type character of the CdSe film which would cause a decrease in space charge layer thickness and manifest itself in a lower I_{sc} but higher V_{oc}.

Fig. 5 shows the V_{oc} of the PEC cells formed with these films as a function of annealing temperature. V_{oc} is almost constant for CdS and CdSe films for

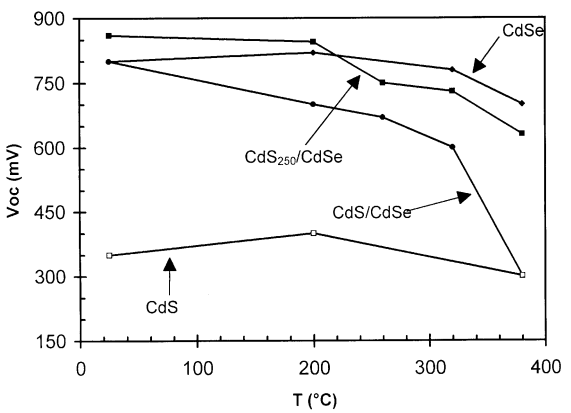

Fig. 5. V_{oc} (open circuit voltage) as a function of annealing temperature for CdS, CdSe and coupled photoanodes. Semiconductor | 0.5 M KOH/0.25 M $K_4Fe(CN)_6$/0.0125 M $K_3Fe(CN)_6$ |C. Illumination intensity of 80 mW/cm^2.

heat-treatment temperatures up to 380°C. At this temperature, the reduction in V_{oc} is less than 20% as compared to that in as prepared films. On the other hand, the coupled films show a faster decay of V_{oc} with annealing temperature. Here again, the coupled CdS_{250}/CdSe film follows more closely the behavior of CdSe at all temperatures, while the CdS/CdSe film annealed at 380°C end up behaving as the CdS film. Changes in fermi levels due to higher donor density (arising from the loss of chalcogenides) will have a strong positive effect on V_{oc}. Surface states which might be formed during air annealing due to oxygen chemisorption will also affect V_{oc}. To a first approximation, however, it is expected that this effect will be similar for CdSe and both coupled films. The deterioration of V_{oc} with annealing temperature for the CdS/CdSe films could be explained by film inversion or photocorrosion of the CdSe layer. The tendency of Se^{2-} to replace S [17], or well, the tendency of CdSe to photocorrode will depend on the amorphousity (bonding) and oxygen content (trapping) of the CdS substrates.

Based on the study of the effect of heat-treatment temperature on I_{sc} and V_{oc}, we select CdS_{250}/CdSe as our deposition method and 280°C as the air annealing temperature for preparing the photoanodes. An aspect to be determined was the nature of the charge separation mechanism of the coupled film and its advantages, if any, over chemically deposited CdSe films. The behavior of the PEC cell formed by this coupled film is shown in Fig. 6. There is an increase in I_{sc}, V_{oc} and cell efficiency (η) with an increase in illumination intensity, which indicates the absence of saturation problems and forecasts higher cell efficiencies with higher illumination intensities. This is an advantage over the photoelectrochemical behavior of a similar system reported by Mahapatra and Dubey [17] in which the reported 4.5% efficiency was limited by saturation. Fig. 7a and Fig. 7b show the linearity of V_{oc} vs. ln I_L (light intensity) and I_{sc} vs. I_L plots. Such linearity is expected from the theory of photovoltaic response of Schottky barriers, which suggests the validity of the Schottky–Mott model [24] for these interfaces.

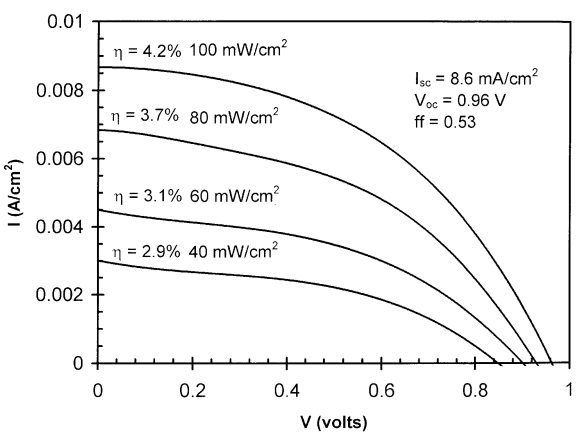

Fig. 6. Current–Voltage characteristics of the CdS_{250}/CdSe photoanode annealed in air at 280°C for 1.5 h. Ferro/ferricyanide electrolyte and variable illumination intensity.

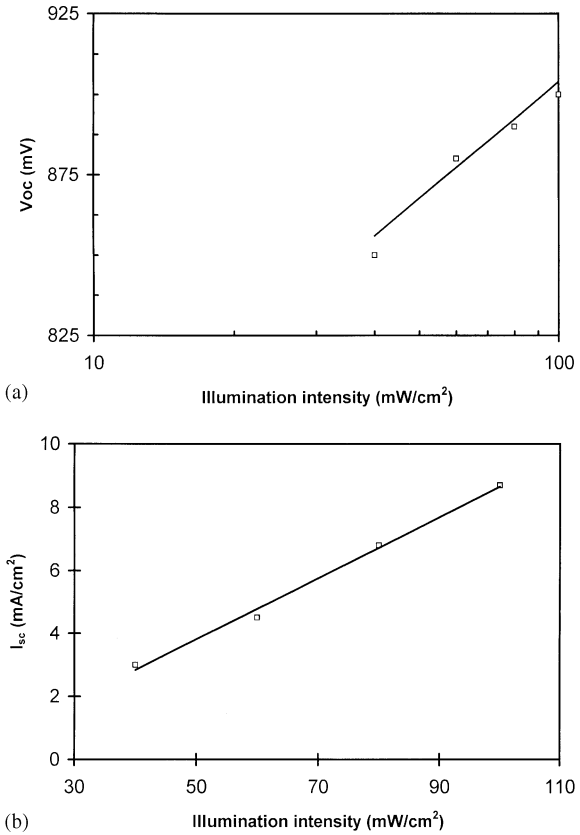

Fig. 7. (a) V_{oc} as a function of ln I_L (illumination intensity) for the system described in Fig. 6., (b) I_{sc} as a function of I_L. The linearity in both curves validate the Schottky–Mott model for this interface.

The stabilities of the CdS_{250}/CdSe and CdSe films are given in Fig. 8. The superior initial stability of the coupled film is clearly seen. At longer operation times (> 3 h) the I_{sc} of both systems is similar and ~ 1 mA/cm^2. The large reduction in I_{sc} at longer times is not only due to photocorrosion and recombination in the semiconducting layer, but also due to polarization in our poorly conducting graphite counter electrode which retards the transfer kinetics at the semiconductor-electrolyte interface. At short operating times, the rectifying nature of the CdS_{250}/CdSe junction could be responsible for its higher stability. In an oversimplified way we can say that the V_{oc} values shown in Fig. 5 indicate that the conducting band of CdS is located roughly 500 mV below the conducting band of CdSe, that is, the photogenerated electrons in the CdSe layer moved down hill to the CdS layer and then to the back contact. In the same way, the photogenerated holes in the CdS layer move towards the more attractive CdSe valence band and then towards the semiconductor-electrolyte interface. It is clear that suppression of charge recombination in coupled

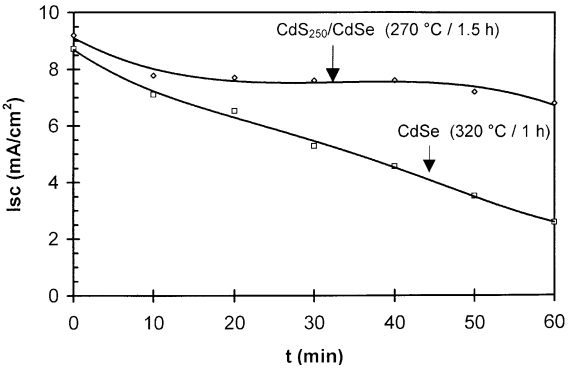

Fig. 8. Photocurrent vs time curve for CdSe air annealed at 320°C for 1 h and CdS_{250}/CdSe air annealed at 280°C for 1.5 h.

semiconductor systems is likely to improve the efficiency of photocurrent generation at short time, but could not overcome the instability at longer times (photocorrosion) due to hole accumulation in the thin CdSe layer. Unless fast charge transfer can be provided, thicker and more electrocatalytic surfaces of CdSe should be implemented.

4. Conclusion

The PEC solar cell characteristics of chemically deposited CdS, CdSe and coupled films formed by consecutive chemical baths of CdS and CdSe were presented, along with their optical and electrical characteristics and the changes brought about in them due to air annealing. The PEC solar cell performance improved with an increase in annealing temperature attaining the best performance for annealing at 320°C. Above such annealing temperature, the performance deteriorated. These trends are very similar for the CdSe and CdS_{250}/CdSe electrodes. The overall improvement achieved in the PEC performance with annealing can be attributed to the increase in crystallinity of the CdSe layer (lower is the E_g, higher the αt) produced by the heat treatment, even though the roles played by oxygen chemisorption and selenium losses are still to be determined. Excellent I–V characteristics were obtained for CdS_{250}/CdSe photoelectrodes annealed at 280°C : V_{oc} of 960 mV, I_{sc} of 8.6 mA/cm^2, fill factor of 0.53 and η of 4.2%. The linearity of V_{oc} versus $\ln(I_L)$ and I_{sc} vs. I_L plots indicates the absence of saturation in the depletion zone and the conservative nature of the numbers presented here. Higher values may be obtained with a better illumination source and/or daylight. The I–V curve remained constant (within 10%) for the coupled electrode and degrades fast for the binary film, when the PEC cells were maintained at the maximum I_{sc} for 1 h. Future work will include studies on the correlation of the PEC performance of the CdS/CdSe photoanodes with their structure and composition before and after photocorrosion in order to elucidate the degradation mechanism.

This would enable one to adapt necessary measures to improve upon the PEC solar cell stabilities.

Acknowledgements

The authors gratefully acknowledge the support received from DGAPA-UNAM and CONACyT, México.

References

[1] M. Graetzel, A.J. McEvoy, in: Proc. 1st World Renewable Energy Congress, vol. 1, 1990, p. 120.
[2] Di Liu, P.V. Kamat, J. Phys. Chem. 97 (1993) 10769.
[3] J. Reichman, M.A. Russak, in: A.J. Nozik (Ed.), Photoeffects at Semiconductor-Electrolyte Interfaces, ACS Symp. Ser., vol. 146, Washington DC, 1981, p. 359.
[4] V. Gotovac, Lj. Aljinovic, M. Lucic'-Lavcevic', Univ. Beograd. Publ. Elektrotehn. Fak., Ser. Teh. fiz. 1 (1991) 63.
[5] V.M. García, M.T.S. Nair, P.K. Nair, R.A. Zingaro, Semicond. Sci. Technol. 10 (1995) 427.
[6] M.T.S. Nair, P.K. Nair, R.A. Zingaro, E.A. Meyers, J. Appl. Phys. 74 (1993) 1879.
[7] M.T.S. Nair, P.K. Nair, R.A. Zingaro, E.A. Meyers, J. Appl. Phys. 75 (1994) 1557.
[8] D.R. Pratt, M.E. Langmuir, R.A. Boudreau, R.D. Rauh, J. Electrochem. Soc. 128 (1981) 1627.
[9] R.A. Boudreau, R.D. Rauh, J. Electrochem. Soc. 130 (1983) 513.
[10] K.C. Mandal, O. Savadogo, J. Mater. Sci. 27 (1992) 4355.
[11] O. Savadogo, K.C. Mandal, Mater. Chem. Phys. 31 (1992) 301.
[12] S. Chandra, R.K. Pandey, R.C. Agrawal, J. Phys. D: Appl. Phys. 13 (1980) 1757.
[13] C.D. Lokhande, S.H. Pawar, Solar Energy Mater 7 (1982) 313.
[14] C.D. Lokhande, S.H. Pawar, Solid State Commun. 49 (1984) 765.
[15] Lj Aljinovic', V. Gotovac, D. Krpan, J. Eng. Phys. 25 (1983) 51.
[16] D. Krpan, V. Gotovac, B. Urli, Electrochim. Acta 29 (1984).
[17] P.K. Mahapatra, A.R. Dubey, Solar Energy Mater. 32 (1994) 29.
[18] D. Lincot, R. Ortega-Borges, J. Electrochem. Soc. 139 (1992) 1880.
[19] R. Ortega-Borges, D. Lincot, J. Electrochem. Soc. 140 (1993) 3464.
[20] J.W. Orton, B.J. Goldsmith, J.A. Chapman, M.J. Powell, J. Appl. Phys. 53 (1982) 1602.
[21] M.V. García-Cuenca, J.L. Morenza, J.M. Codina, J. Phys. D 20 (1987) 51.
[22] J.L. Botto, A.M. Ramis, I.B. Schalamuk, M.A. Sánchez, Thermochimica Acta 249 (1995) 325.
[23] S. Perkowitz, Optical Characterization of Semiconductors: Infrared, Raman, and Photoluminescence Spectroscopy, Academic Press, San Diego, CA, 1993.
[24] T.S. Moss, G.J. Burrel, B. Ellis, Semiconductor Opto-Electronics, Butterworths, London, 1973.